2020 IEEE/RSJ International Conference on Intelligent Robots and Systems (IROS)
October 25-29, 2020, Las Vegas, NV, USA (Virtual)

Ultra-Wideband Aided UAV Positioning Using Incremental Smoothing with Ranges and Multilateration

Jungwon Kang[1], Kunwoo Park[1], Zahra Arjmandi[1], Gunho Sohn[1]
Mozhdeh Shahbazi[2] and Patrick Ménard[2]

***Abstract*— In this paper, we present a novel smoothing approach for ultra-wideband (UWB) aided unmanned aerial vehicle (UAV) positioning. Existing works based on smoothing or filtering estimate 3D position of UAV by updating a solution for each single 1D low-dimensional UWB range measurement. However, a low-dimensional single range measurement merely acts as a weak constraint in a solution space for UAV position estimation, and thus it can often lead to incorrect estimation in unfavorable conditions. Inspired by the idea that the multilateration outcome can be utilized as a measurement providing a strong constraint, we utilize two types of UWB-based measurements: (i) each single 1D range as a high-rate measurement with a weak constraint, and (ii) multilateration outcome as a low-rate measurement with a strong constraint. We propose an incremental smoothing-based method that seamlessly integrates these two types of UWB-based measurements and inertial measurement into a unified factor graph framework. Through experiments under a variety of scenarios, we demonstrate the effectiveness of the proposed method.**

I. INTRODUCTION

Recent advances in technology for unmanned aerial vehicles (UAVs) such as quadcopters have facilitated the application of UAVs for inspecting and monitoring infrastructures. In these applications, positioning a UAV in a given space is the critical capability for performing essential tasks such as mapping and navigation. The challenges lie in operations in global navigation satellite system (GNSS)-denied environments, e.g., inside chimney [1] and tunnel [2].

An emerging solution for operation in GNSS-denied environments is to use ultra-wideband (UWB) sensors [3] as an alternative to GNSS. The UWB sensors can form a radio frequency-based sensor network, where some sensor modules are placed as anchors and one module is attached as a tag to the vehicle. In this configuration, by leveraging Time of Flight (ToF) techniques such as Time Difference of Arrival (TDoA) and Two-Way Ranging (TWR), the UWB tag can get range between the tag and each anchor in a round-robin manner. The large bandwidth of UWB signal enables the UWB signal to be robust to multipath and non-line-of-sight (NLOS) effects, and thus distances can be measured up to a few hundreds meter with centimeter-level accuracy. Because of these strong points, UWB sensors have gained popularity as a positioning sensor in GNSS-denied environments [4]–[6].

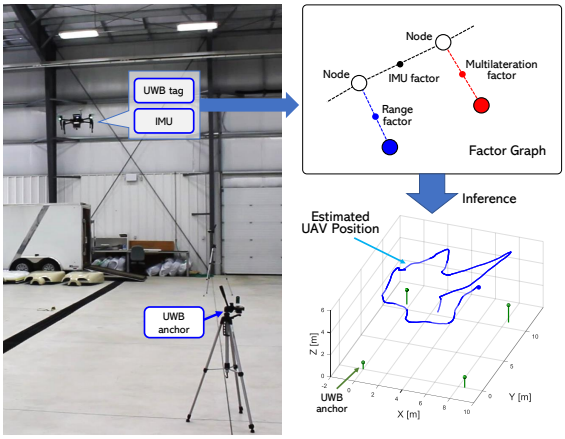

Fig. 1. Description of the proposed method for UAV positioning based on incremental smoothing which seamlessly integrates two types of UWB-based measurements and inertial measurement into a unified factor graph framework. Here, a node indicates a state to be estimated, i.e., UAV position.

The positioning of UAV using UWB sensors has been often addressed as a problem of estimating 3D position of UAV from UWB range and additional inertial measurements. To tackle the estimation problem, the extended Kalman filter (EKF) has been widely used in many works [7]–[10]. In addition to the above *filtering*-based methods, some recent works [4], [5], [11], [12] have presented *smoothing*-based approach, in which the estimation problem is dealt with by graph optimization. These existing methods estimate the 3D position of UAV by updating a solution for each single 1D low-dimensional UWB range measurement. Here, we point out that a low-dimensional single range measurement merely acts as a weak constraint in a solution space for the UAV position estimation, and thus it can often lead to incorrect estimation in unfavorable conditions.

Meanwhile, like other anchor-based systems such as GNSS, multilateration [13]–[16] can be applied to UWB system. Although the multilateration is only applicable to a set of range data that meets certain conditions, the multilateration directly produces the 3D position of UAV. Our work was inspired by the idea that the multilateration outcome can be utilized as a measurement providing directly 3D position of UAV, i.e., a strong hint for the position, in the filtering or smoothing approaches. It means that the multilateration

[1]Jungwon Kang, Kunwoo Park, Zahra Arjmandi and Gunho Sohn are with the Department of Earth and Space Science and Engineering, Lassonde School of Engineering, York University, 4700 Keele Street, Toronto, Ontario M3J 1P3, Canada kctown99@gmail.com, kwparkv@gmail.com, zahraarj@yorku.ca, gsohn@yorku.ca

[2]Mozhdeh Shahbazi and Patrick Ménard are with Centre de géomatique du Québec, Saguenay, Québec G7H 1Z6, Canada mshahbazi@cgq.qc.ca, pmenard@cgq.qc.ca

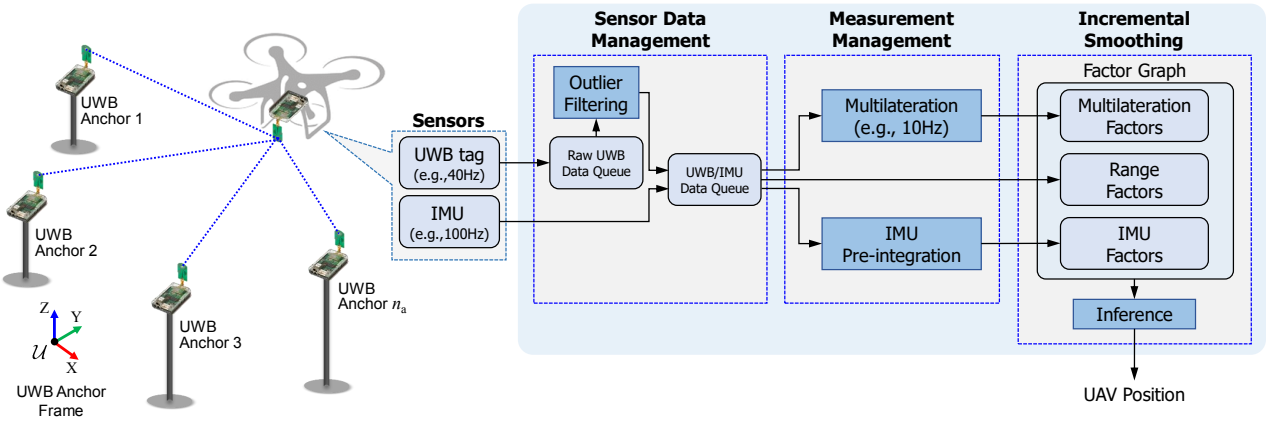

Fig. 2. An overview of the proposed system.

outcome can be used as a strong constraint in a solution space for finding a solution. Hence, each single 1D range can be used as a high-rate measurement with a weak constraint, and the multilateration outcome can be utilized as a low-rate measurement with a strong constraint.

In this work, we present a method for UAV positioning based on *incremental smoothing*, which seamlessly integrates two types of UWB-based measurements and inertial measurement into a unified factor graph framework, as described in Fig. 1. Our major contributions are as follows:

- We present a method for multilateration that computes an algebraic solution, followed by a non-linear optimization.
- We propose an *incremental smoothing* approach that seamlessly integrates each single range measurement, multilateration-based 3D position of UAV and inertial measurement into a unified framework using a factor graph. Furthermore, we also propose a novel strategy for adding a multilateration factor into a graph for online operation.
- We conducted experiments under a variety of scenarios in a GNSS-denied environment to demonstrate the effectiveness of the proposed method.

II. System Overview

The overview of the proposed system is depicted in Fig. 2, and it can be described by UWB anchors, sensor data and UAV positioning algorithm.

A. UWB Anchors

In our system, we suppose that at least four UWB anchors are placed at each different fixed position. Practically, the anchors need to be spread evenly in a given area. Let $\mathcal{U}$ be the UWB anchor frame, which can be located on a location for one of anchors. The position of each anchor in the frame $\mathcal{U}$ is assumed to be known in advance, in which it can be done by solving linear equations for anchor positions using measured distances between anchors [10]. Here, the position of ith anchor in the frame $\mathcal{U}$ is denoted by $\mathbf{p}_{\mathrm{ua},i} = [x_{\mathrm{ua},i}, y_{\mathrm{ua},i}, z_{\mathrm{ua},i}]$.

B. Sensor Data

We get sensor data from UWB tag and IMU installed on UAV. First, we get range data between UWB tag and UWB anchors in a round-robin manner, i.e., a range between the tag and each anchor is acquired alternately. Here, a range between the UWB tag and UWB anchor i is denoted by $r^k_{\mathrm{ua},i}$, where k is a time step for acquisition of the data. When it comes to the IMU data, we get several kinds of data including linear acceleration $\boldsymbol{\alpha}^k$, angular velocity $\boldsymbol{\omega}^k$ and height h^k. Note that UWB and IMU data can be acquired at different frequencies.

C. UAV Positioning from Sensor Data

Given the sensor data, UAV positioning is done by three parts: (i) sensor data management, (ii) measurement management and (iii) incremental smoothing part including construction of a factor graph and estimation of UAV position on the factor graph.

First, in sensor data management part, raw UWB data is stored in the queue called *raw UWB data queue*, where the queue stores raw UWB data over some frames, i.e., from the past frame to now, for each anchor. Then, outliers in the raw data are filtered out by the outlier filtering method described in Section III. The filtered UWB data and IMU data are stored in another queue called *UWB/IMU data queue*, where the queue stores filtered UWB data and IMU data over some frames, i.e., from the past frame to the present. Second, in measurement management part, measurements are generated by (i) multilateration presented in Section IV, (ii) a single UWB range, and (iii) IMU pre-integration [17] from the sensor data in the UWB/IMU data queue. In the last part, factors for each measurement of multilateration, single range and IMU data are created. With the created factors, a factor graph is updated by the update method presented in Section V. The inference [18] on the factor graph produces UAV position in the form of a trajectory including current position as well as the past ones.

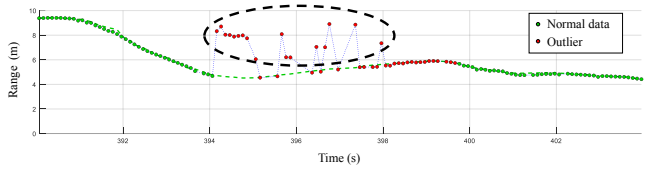

Fig. 3. Acquired range over time between a UWB tag and a certain UWB anchor, and the result of the proposed outlier filtering algorithm, where the result is represented by color (green: normal data, red: outlier) in each data. The set of data in the dashed circle indicate true outliers trapped in NLOS cases.

III. Filtering out Outliers in UWB Range Data

As described in Fig. 2, every incoming UWB range data from a UWB tag is stored in the raw UWB data queue, and then it is checked if it is an outlier. In [8], [11], an outlier is detected by checking the difference between expected range and measured one. However, this outlier detection method heavily relies on the expected vehicle position to compute the expected range, which can be erroneous if the expected position is incorrect. Hence, we sought to detect outliers without relying on the expected vehicle position. As indicated in Fig. 3, we found there is substantial fluctuation over time around outliers. Here, based on this observation, we classify a range data into normal data or outlier, according to range variation over time. A range data is classified into an outlier if it has large variation in the temporal section.

Given a newly incoming range $r^k_{\mathrm{ua},i}$ acquired from anchor i at the time step k, we get range variation between a pair of two consecutive data in a temporal sliding window. As a range variation, we compute absolute difference in range values of two consecutive data. Let S_w be the size of the temporal sliding window. Then, we get a total of $(S_\mathrm{w}-1)$ range variation values. The data is classified as normal one if all the range variation values are below R_o, where R_o is a value for defining a large range variation. Then, it is stored in the UWB/IMU data queue. Otherwise, the data is considered an outlier, and it is not used for further process. Fig. 3 shows an example result of our outlier filtering algorithm, where we used $S_\mathrm{w}=15$ and $R_\mathrm{o}=0.7m$. Due to the classification using a temporal sliding window, our algorithm could produce results with a high recall for outlier detection.

IV. Multilateration for Direct Measurement of UAV Position

In this section, we present an algorithm for multilateration. With a set of range data supposed to be acquired at the same time and known positions of anchors, the multilateration produces a 3D position of the UWB tag in the frame $\mathcal{U}$. However, in our case, we use a set of the data acquired within a short interval of time, as it can not be acquired at the exact same time. Among the UWB range data in the UWB/IMU data queue, we pick m data ($m \geq 4$), each of which is the latest data for an anchor. Given these m data, we compute the time difference between the newest data and the oldest one. Only when the time difference is below T_d which is small one (e.g., $T_\mathrm{d}=0.1s$), we run the multilateration with these m data.

The proposed multilateration algorithm consists of obtaining an algebraic solution and the following non-linear optimization:

1) Obtaining an initial position by recursive least squares: In order to produce an initial solution for the position, we adopted the method [14] that uses recursive least squares based on the algebraic constraint. We denote the 3D position of the UWB tag by $\mathbf{x}_\mathrm{mlat} = [x_\mathrm{mlat}, y_\mathrm{mlat}, z_\mathrm{mlat}]$. From $\|\mathbf{x}_\mathrm{mlat}-\mathbf{p}_{\mathrm{ua},i}\|_2^2 = (r_{\mathrm{ua},i})^2$, we can build the equation $\mathbf{A}\mathbf{x}_\mathrm{mlat} = \mathbf{b}$, where each row of $\mathbf{A}$ is given by $[1, -2x_{\mathrm{ua},i}, -2y_{\mathrm{ua},i}, -2z_{\mathrm{ua},i}]$ and the corresponding row of $\mathbf{b}$ is $[(r_{\mathrm{ua},i})^2-(x_{\mathrm{ua},i})^2-(y_{\mathrm{ua},i})^2-(z_{\mathrm{ua},i})^2]$. By solving the above equation, we can get a 3D position $\mathbf{x}_\mathrm{mlat}$ of the UWB tag in the frame $\mathcal{U}$.

2) Refining the initial position by non-linear optimization: We refine the initial solution by the Levenberg-Marquardt non-linear optimization. We build the objective function including geometric constraints between the UWB tag and anchors. Meanwhile, in a certain case (e.g., our case described in Section VI-B) where UWB anchors are almost coplanar, the solution ambiguity can happen along the height direction, as described in our previous work [19]. Here, in order to overcome this issue, we add an additional term for taking account of a height measurement from IMU. Finally, we get the refined solution by solving

$$\hat{\mathbf{x}}_\mathrm{mlat} = \arg\min_{\mathbf{x}_\mathrm{mlat}} \lambda \cdot e_\mathrm{h}^2 + \sum\nolimits_{i\in m} (e_{\mathrm{ua},i})^2 \qquad (1)$$

where $e_\mathrm{h} = h - z_\mathrm{mlat}$ and $e_{\mathrm{ua},i} = r_{\mathrm{ua},i} - \|\mathbf{x}_\mathrm{mlat}-\mathbf{p}_{\mathrm{ua},i}\|_2$. Here, λ is a parameter for weighting. Here, considering the accuracy of each sensor, we used $\lambda = 0.1$.

V. UAV Positioning Using Factor Graph

In this section, we describe how a factor graph for estimating the UAV position is constructed from each measurement. First, we briefly review the factor graph framework. Then, we describe factors for each measurement. Lastly, we propose a method of updating a factor graph for online operation. Here, we estimate the 3D position of UWB tag, as UAV position, in the UWB anchor frame $\mathcal{U}$. In addition, we suppose IMU is located close to the UWB tag.

A. Factor Graph Framework

To estimate 3D position of UAV, we were motivated by a factor graph-based incremental smoothing framework [20], as it enables us to handle asynchronous sensor measurements having different frequencies and it can also easily accommodate the addition of a new type of a measurement. In the factor graph framework, a factor graph encoding the connectivity between states to be estimated and available measurements is constructed. Each measurement can form a factor, which is added to the graph. Let $\mathbf{x}$ be the set of all states to be estimated, $\mathbf{x}_i$ be a subset of $\mathbf{x}$, and $f_i(\mathbf{x}_i)$ be a factor for $\mathbf{x}_i$. Assuming a Gaussian noise model, the

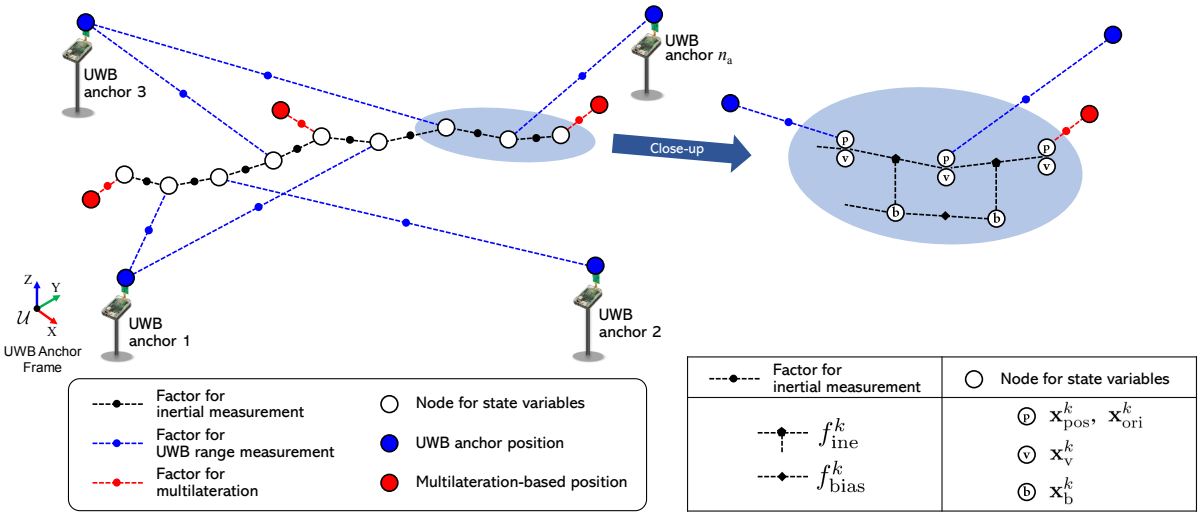

Fig. 4. Factor graph representation of the proposed algorithm. In the proposed algorithm, we have the state variables over time for UAV position $\mathbf{x}^k_{\text{pos}}$, orientation $\mathbf{x}^k_{\text{ori}}$, velocity $\mathbf{x}^k_{\text{v}}$ of the UAV, and biases $\mathbf{x}^k_{\text{b}}$ for an accelerometer and a gyroscope of the IMU. The measurements and the state variables are associated by factors. Here, we used three types of factors to handle multilateration-based position, single UWB range, and inertial measurements, respectively.

Fig. 5. Description of the *add-after-eliminating* strategy for adding a multilateration factor to the factor graph.

$f_i(\mathbf{x}_i)$ is represented by $\exp(-\frac{1}{2}\left\|h_i(\mathbf{x}_i)-\mathbf{z}_i\right\|^2_{\Sigma_i})$, where $\mathbf{z}_i$ is a measurement, $h_i(\cdot)$ is a measurement function and Σ_i is the covariance matrix. The $f_i(\mathbf{x}_i)$ can be also represented by $\exp(-\frac{1}{2}\left\|h_i(\mathbf{x}_{i_1},\mathbf{z}_i)-\mathbf{x}_{i_2}\right\|^2_{\Sigma_i})$, where $\mathbf{x}_{i_1}$ and $\mathbf{x}_{i_2}$ are two different subsets of $\mathbf{x}_i$. If a measurement is available, the corresponding factor $f_i(\mathbf{x}_i)$ can be added to the graph. The factor graph represents a whole objective function for the estimation, where each factor represents a sub-function in the objective function. Here, calculating the maximum a posteriori (MAP) estimate of the posterior probability of the states is equivalent to performing inference over the factor graph. An efficient incremental inference algorithm over the factor graph, iSAM2 [18], can be applied to get the optimal states $\hat{\mathbf{x}}$:

$$\hat{\mathbf{x}} = \arg\min_{\mathbf{x}} \prod_i f_i(\mathbf{x}_i) \tag{2}$$

The 3D position of UAV can be obtained by calculating the MAP estimate of the posterior probability of the states including position, orientation, velocity, biases over time, given all available measurements. In this problem, the state variables at the time step k include (i) position $\mathbf{x}^k_{\text{pos}}$ in the UWB anchor frame $\mathcal{U}$, (ii) orientation $\mathbf{x}^k_{\text{ori}}$ in the frame $\mathcal{U}$, (iii) the velocity $\mathbf{x}^k_{\text{v}}$ of the UAV in frame $\mathcal{U}$, and (iv) the biases $\mathbf{x}^k_{\text{b}}$ for an accelerometer and a gyroscope of the IMU.

B. Factors

In our algorithm, we use the following three types of factors. Here, we simply use $d(\cdot)$ to denote $f_i(\mathbf{x}_i)$.

1) Factor for single UWB range measurement: This factor is created from single range measurement, and it is given as

$$f^k_{\text{range}}(\mathbf{x}^k_{\text{pos}}) \doteq d(\left\|\mathbf{x}^k_{\text{pos}} - \mathbf{p}_{\text{ua},i}\right\|_2 - r^k_{\text{ua},i}) \tag{3}$$

2) Factor for multilateration-based measurement: This factor is generated from multilateration-based position measurement, and it is given as

$$f^k_{\text{mlat}}(\mathbf{x}^k_{\text{pos}}) \doteq d(\mathbf{x}^k_{\text{pos}}, \mathbf{x}^k_{\text{mlat}}) \tag{4}$$

where $\mathbf{x}^k_{\text{mlat}}$ is the multilateration outcome at time step k, and it is obtained by a multilateration method presented in Section IV.

3) Factor for inertial measurement: This factor is created from the incremental motion obtained from measurements of linear acceleration, angular velocity of the IMU. To handle the high-rate operation of the IMU, we adopt the IMU pre-integration technique [17], and introduce the equivalent IMU factor that represents several consecutive IMU measurements. Thus, instead of adding factors to the factor graph at IMU rate, the factors are added at a lower frequency that is determined by other sensors e.g., UWB sensor.

Let $\mathbf{x}^{k^-}_{\text{pvb}}$ denote $[\mathbf{x}^{k^-}_{\text{pos}}, \mathbf{x}^{k^-}_{\text{ori}}, \mathbf{x}^{k^-}_{\text{v}}, \mathbf{x}^{k^-}_{\text{b}}]$, and $\mathbf{x}^k_{\text{pv}}$ indicates $[\mathbf{x}^k_{\text{pos}}, \mathbf{x}^k_{\text{ori}}, \mathbf{x}^k_{\text{v}}]$. where k^- is a previous time step that a pre-integration began, such that $k^- < k$. Then, we create the following two factors:

$$f^k_{\text{ine}}(\mathbf{x}^{k^-}_{\text{pvb}}, \mathbf{x}^k_{\text{pv}}) \doteq d(\mathbf{x}^k_{\text{pv}} - h(\mathbf{x}^{k^-}_{\text{pvb}}, \Delta\mathbf{x}_{k^-,k})) \tag{5}$$

$$f^k_{\text{bias}}(\mathbf{x}^{k^-}_{\text{b}}, \mathbf{x}^k_{\text{b}}) \doteq d(\mathbf{x}^k_{\text{b}} - g(\mathbf{x}^{k^-}_{\text{b}})) \tag{6}$$

Algorithm 1 Online Operation of UAV Positioning

Initialization: Factors $\mathcal{F} = \{\}$, States $\mathcal{S} = \{\}$
while measurement $\mathbf{z}^k$ **do**
  if $\mathbf{z}^k$ is an inertial measurement **then**
    Perform IMU pre-integration.
  else if $\mathbf{z}^k$ is $r^k_{\mathrm{ua},i}$ **then**
    if $\exists$ IMU pre-integrated values **then**
      Create f^k_{ine}, f^k_{bias} by (5) and (6).
    end if
    if Multilateration can be applied **then**
      Eliminate range factors and IMU factors in $\mathcal{F}$ related to the multilateration.
      Create f^k_{mlat} by (4).
      Create f^k_{ine}, f^k_{bias}
    else
      Create f^k_{range} by (3).
    end if
    Add factors to $\mathcal{F}$.
    Add states to $\mathcal{S}$.
  end if
  if Incremental smoothing is available **then**
    Perform an incremental inference using [18].
    Retrieve estimated states.
  end if
end while

where $\Delta\mathbf{x}_{k^-,k}$ indicates the relative motion from k^- to k that is obtained from the pre-integration of inertial measurement, and $g(\mathbf{x}_{\mathrm{b}}^{k^-})$ is a random walk model.

C. Online Operation of UAV Positioning

Here, we present a novel strategy for online operation of UAV positioning with the aforementioned factors. For a newly incoming range stored in the UWB/IMU data queue, we check if the multilateration can be applied, by the short time interval condition, to m data $(m \geq 4)$ in the UWB/IMU data queue, where m data include the newly incoming range and the latest $m-1$ ranges from other anchors. If the multilateration is not available, a range factor is simply created and added to the graph. On the other hand, if the multilateration can be applied, a multilateration factor is created. However, if the multilateration factor is added to the graph, it leads to the violation of the factor graph condition that all factors should be independent, as ranges from other anchors used for multilateration were already utilized for range factors.

To overcome the above issue, we propose a method, named *add-after-eliminating* strategy, for adding the multilateration factor into a graph without the violation of the factor graph condition. In this strategy, given the multilateration outcome, range factors and IMU factors related to ranges for the multilateration are eliminated in the graph, and then the multilateration factor and newly created IMU factor are added to the graph, as described in Fig. 5. By this strategy, all factors keep independent. We indicate that, in the proposed method, a range is used for only one factor.

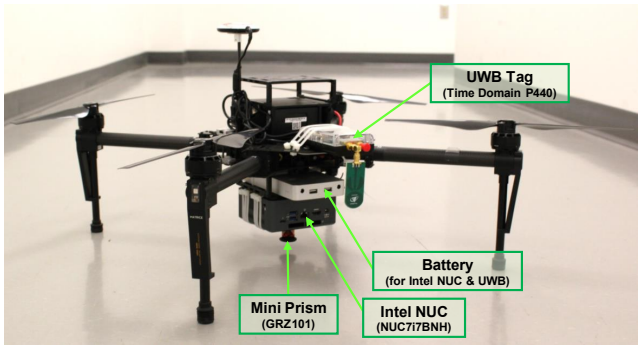

Fig. 6. Our UAV system which is a quadcopter equipped with a UWB tag. The flight controller with an IMU is located at the center of the quadcopter.

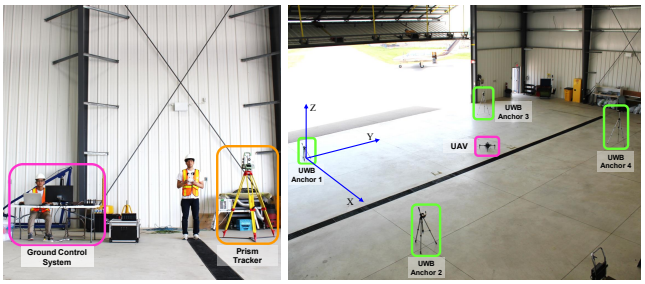

Fig. 7. Experimental environment: ground control system and prism tracker (left), experimental setup (right)

The whole procedure for online operation is depicted in Algorithm 1, and Fig. 4 illustrates the created factor graph.

VI. Experimental Results

In this section, we first describe our UAV system and experimental setup. Then, we present experimental results and discussion on the results.

A. UAV System and UWB Sensor

Our UAV system is built on DJI M100 quadcopter, as shown in Fig. 6. At the bottom of the UAV, we installed an Intel NUC, a UWB tag and a battery as payload. In addition, at the center bottom of the UAV, we attached a 360° mini prism for obtaining the ground-truth position of the vehicle. As UWB sensors, we used a total of five Time Domain PulsON 440 UWB modules, where a range can be obtained up to a few hundred meter with 20mm accuracy in clear line-of-sight scenarios. Among them, one module was used as a UWB tag installed on the UAV, and other four modules were used as UWB anchors.

Sensor data acquisition software was implemented using ROS kinetic on Ubuntu 16.04. From IMU of the UAV, we could get data including linear acceleration, angular velocity, and height at 100 Hz. To get UWB range data, the UWB tag sends distance request to anchors in a round-robin manner. For each anchor, we got the range data at 10 Hz, resulting in 40 Hz from all the four anchors. In addition, we used the GTSAM library [21] to implement our positioning algorithm.

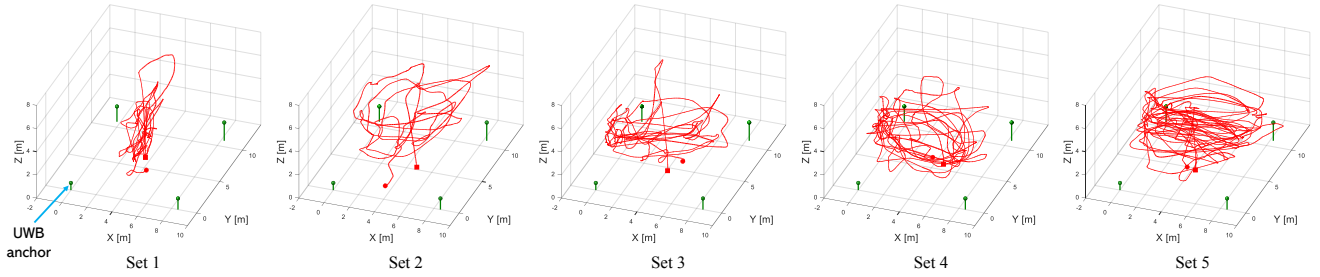

Fig. 8. Ground-truth trajectories for each set in the dataset, where a square and a circle in each figure indicate a starting point and an ending point, respectively.

TABLE I
DESCRIPTION OF THE DATASET

Set	Duration	Distance travelled	x-min x-max	y-min y-max	z-max
Set 1	175.733s	138.831m	2.592m 4.745m	1.779m 12.689m	6.910m
Set 2	212.171s	167.494m	-0.281m 8.164m	-1.356m 13.082m	6.087m
Set 3	241.269s	210.485m	-0.474m 7.916m	-0.030m 9.970m	7.164m
Set 4	363.491s	298.466m	-0.440m 8.256m	0.207m 8.474m	6.212m
Set 5	394.531s	448.229m	-1.403m 9.390m	-1.184m 10.174m	5.347m

B. Experimental Setup

We conducted experiments in a cuboid-shaped indoor space, as shown in Fig. 7, whose size is 26m (width) $\times$ 33m (length) $\times$ 10m (height), where the GNSS is completely denied. In the given area, we installed four UWB anchors, and the (x, y, z) position of the anchors was (0.00, 0.00, 0.62), (8.51, 0.00, 0.96), (-0.26, 10.77, 1.32), (8.25, 10.84, 1.58), respectively, where the unit is meter. In addition, in order to obtain the ground-truth position of the UAV, we used the Leica Nova MS60 MultiStation as prism tracker and tracked the prism attached on the UAV using the automatic target recognition functionality of the MultiStation. It provided the 3D tracked position with mm-level accuracy at 10Hz.

The acquired dataset is summarized in Table I, and trajectories of each set are presented in Fig. 8. We acquired a total of five sets by manually driving the UAV. As shown in Fig. 8, each set includes severe lateral motions and up-and-down motions as well.

C. Results on Multilateration

1) Result: First, we evaluated the proposed multilateration method on the acquired dataset. For comparison study, we also ran the baseline method [14] that uses recursive least squares based on the algebraic constraint. As stated earlier, we run the multilateration only when the time difference of given four data is below $T_{\mathrm{d}} = 0.1s$. Thus, we could get the multilateration results from 15.95% of total time steps in the dataset. Table II describes the multilateration results of the two methods. We used the mean absolute error (MAE) to measure the error.

2) Discussion: As indicated in Table II, the proposed multilateration entirely outperformed the baseline method. The baseline method produced large errors in z values due to the solution ambiguity along the height direction. On the other hand, the proposed multilateration method could avoid such an ambiguity by incorporating the height measurement from IMU into the multilateration.

D. Result on Positioning

1) Result: We also evaluated the proposed positioning method on the acquired dataset. We compared the performance of the proposed positioning method and the baseline one, where the baseline method uses only two factors for single range and inertial measurements without the use of factors for multilateration. Table III presents the MAE errors for the two methods. Figure 9 shows the positioning results on Set 5 that has the largest duration and distance travelled.[1]

2) Discussion: As indicated in Table III, the proposed method was slightly better than the baseline one, in the first four sets. However, a clear distinction between the proposed method and the baseline in terms of accuracy can be seen in Set 5 that is the most challenging set due to its long operation time and distance travelled with large motion change. The baseline method failed correct estimation in the section with large motion change, while the proposed method could work properly even under such a challenging section by means of the integration of multilateration in the estimation. From these experiments, we could see that the integration of multilateration clearly helped produce better results in terms of accuracy and robustness.

VII. Conclusions and Future Works

We proposed an incremental smoothing-based method that seamlessly integrates these two types of UWB-based measurements and inertial measurement into a unified factor graph framework. In the proposed method, besides each single range as a high-rate measurement, we also used multilateration outcome as a low-rate measurement acting as a strong constraint in a solution space. Moreover, we also presented an online operation strategy for adding a

[1]The result video for all five sets is available at `https://github.com/yorku-ausml/qdrone`.

TABLE II

THE MEAN ABSOLUTE ERROR OF MULTILATERATION OUTCOMES (UNIT: METER),

WHERE THE RESULTS ARE OBTAINED FROM 15.95% OF THE WHOLE TIME STEPS IN THE DATASET.

-	-	Set 1	Set 2	Set 3	Set 4	Set 5	Mean
Baseline multilateration [14]	x	0.045	0.066	0.065	0.056	0.088	0.064
	y	0.070	0.090	0.089	0.065	0.088	0.080
	z	0.612	0.846	0.749	0.651	0.932	0.758
	xyz	0.633	0.876	0.782	0.669	0.967	0.785
Proposed multilateration	x	**0.032**	**0.042**	**0.053**	**0.043**	**0.074**	**0.049**
	y	**0.045**	**0.049**	**0.056**	**0.038**	**0.047**	**0.047**
	z	**0.113**	**0.112**	**0.088**	**0.126**	**0.106**	**0.109**
	xyz	**0.141**	**0.145**	**0.139**	**0.151**	**0.162**	**0.148**

TABLE III

THE MEAN ABSOLUTE ERROR OF ESTIMATED POSITIONS (UNIT: METER),

WHERE THE RESULTS ARE OBTAINED FOR THE WHOLE TIME STEPS IN THE DATASET.

-	-	Set 1	Set 2	Set 3	Set 4	Set 5	Mean
Baseline positioning	x	**0.032**	**0.035**	**0.048**	**0.043**	0.116	0.055
	y	0.059	**0.047**	0.061	0.044	0.139	0.070
	z	0.315	0.145	0.212	0.273	1.418	0.473
	xyz	0.338	0.171	0.251	0.294	1.457	0.502
Proposed positioning	x	**0.035**	0.045	0.060	0.045	**0.073**	**0.052**
	y	**0.068**	0.049	**0.058**	**0.042**	**0.075**	**0.058**
	z	**0.238**	**0.134**	**0.169**	**0.177**	**0.021**	**0.186**
	xyz	**0.270**	**0.164**	**0.215**	**0.202**	**0.273**	**0.225**

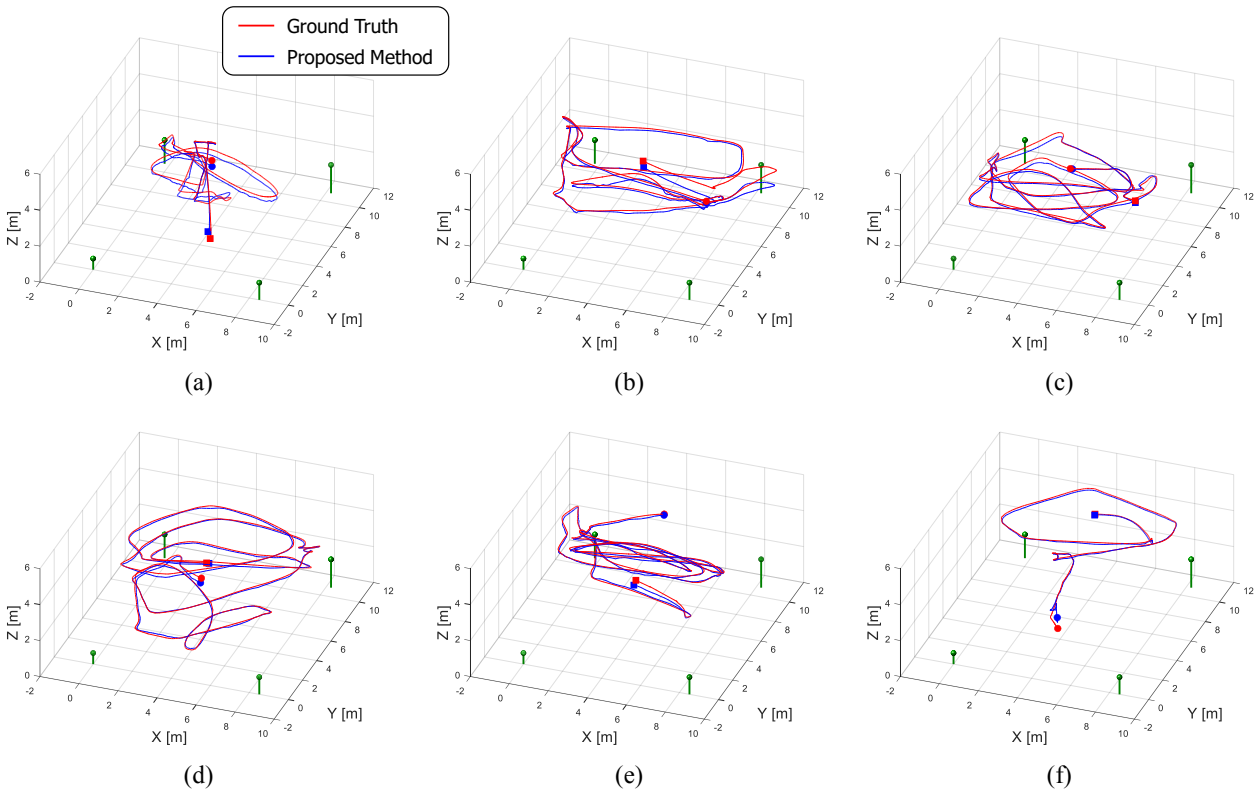

Fig. 9. Estimated positions by the proposed method, showing results on Set 5 in the section of (a) 0.0s to 70.0s, (b) 70.0s to 140.0s, (c) 140.0s to 210.0s, (d) 210.0s to 280.0s, (e) 280.0s to 350.0s and (f) 350.0s to the end. Here, a square and a circle in each figure indicate a starting point and an ending point, respectively.

multilateration factor into a graph without the violation of the factor graph condition. Through experiments under a variety of scenarios, we demonstrated the effectiveness of the proposed method.

However, there are several issues that we need to address for further development. First, the problem of properly setting values of the uncertainty for a multilateration factor has not yet been fully addressed. In this work, we derived a covariance matrix from the multilateration result described in Section VI-C, and used the covariance matrix for all the multilateration factors. However, we need to further develop a method for determining the uncertainty values more precisely, taking account of factors (e.g., the dilution of precision [22], [23]) that can affect the uncertainty of multilateration outcomes. In addition, we also need to further validate the proposed method through more extensive experiments in various environments [24].

REFERENCES

[1] M. Nieuwenhuisen, J. Quenzel, M. Beul, D. Droeschel, S. Houben, and S. Behnke, "ChimneySpector: Autonomous MAV-based indoor chimney inspection employing 3D laser localization and textured surface reconstruction," *International Conference on Unmanned Aircraft Systems (ICUAS)*, 2017.

[2] W. Zhen and S. Scherer, "Estimating the localizability in tunnel-like environments using LiDAR and UWB," *IEEE International Conference on Robotics and Automation (ICRA)*, 2019.

[3] A. Alarifi, A. Al-Salman, M. Alsaleh, A. Alnafessah, S. Al-Hadhrami, M. A. Al-Ammar, and H. S. Al-Khalifa, "Ultra wideband indoor positioning technologies analysis and recent advances," *Sensors*, vol. 16, no. 5, 2016.

[4] C. Wang, H. Zhang, T.-M. Nguyen, and L. Xie, "Ultra-wideband aided fast localization and mapping system," *IEEE/RSJ International Conference on Intelligent Robots and Systems (IROS)*, 2017.

[5] F. J. Perez-Grau, F. Caballero, L. Merino, and A. Viguria, "Multi-modal mapping and localization of unmanned aerial robots based on UWB and RGB-D sensing," *IEEE/RSJ International Conference on Intelligent Robots and Systems (IROS)*, 2017.

[6] C. Kanellakis, et al., "Autonomous visual inspection of large-scale infrastructures using aerial robots," *arXiv:1901.05510v1*, 2019.

[7] M. W. Mueller, M. Hamer and R. D'Andrea, "Fusing ultra-wideband range measurements with accelerometers and rate gyroscopes for quadcopter state estimation," *IEEE International Conference on Robotics and Automation (ICRA)*, 2015.

[8] K. Guo, Z. Qiu, C. Miao, A. H. Zaini, C.-L. Chen, W. Meng and L. Xie, "Ultra-wideband-based localization for quadcopter navigation," *Unmanned Systems*, vol. 4, no. 1, pp. 23-34, 2016.

[9] E. Fresk, K. Ödmark and G. Nikolakopoulos, "Ultra wideband enabled inertial odometry for generic localization," *IFAC-PapersOnLine*, 2017.

[10] B. Dewberry and M. Einhorn, "Indoor aerial vehicle navigation using ultra wideband active two-way ranging," *XPONENTIAL*, 2016.

[11] C. Wang, X. Fang, T.-M. Nguyen and L. Xie, "Graph optimization approach to localization with imu and ultra-wideband measurements," *arXiv:1802.10276*, 2018.

[12] E. Strömberg, "Smoothing and mapping of an unmanned aerial vehicle using ultra-wideband sensors," *Master Thesis, KTH*, 2017.

[13] Y. Zhou, J. Li, and L. Lamont, "Multilateration localization in the presence of anchor location uncertainties," *IEEE Global Communications Conference (GLOBECOM)*, 2012.

[14] A. Norrdine, "An algebraic solution to the multilateration problem," *International Conference on Indoor Positioning and Indoor Navigation*, 2012.

[15] J. Li, X. Yue, J. Chen and F. Deng, "A novel robust trilateration method applied to ultra-wide bandwidth location systems," *Sensors*, vol. 17, no. 4, 2017.

[16] P. Cotera, M. Velazquez, D. Cruz, L. Medina and M. Bandala, "Indoor robot positioning using an enhanced trilateration algorithm," *International Journal of Advanced Robotic Systems*, vol. 13, no. 3, 2016.

[17] T. Lupton and S. Sukkarieh, "Visual-inertial-aided navigation for high-dynamic motion in built environments without initial conditions," *IEEE Transactions on Robotics*, vol. 28, no. 1, pp. 61-76, 2012.

[18] M. Kaess, H. Johannsson, R. Roberts, V. Ila, J. Leonard, and F. Dellaert, "iSAM2: incremental smoothing and mapping using the Bayes tree," *International Journal of Robotics Research*, vol. 31, no. 231, pp. 217-236, 2012.

[19] K. Park, J. Kang, Z. Arjmandi, M. Shahbazi, and G. Sohn, "Multilateration under flip ambiguity for UAV positioning using ultrawide-band," *ISPRS Congress*, 2020.

[20] V. Indelman, S. Williams, M. Kaess, and F. Dellaert, "Information fusion in navigation systems via factor graph based incremental smoothing," *Robotics and Autonomous Systems*, vol. 61, no. 8, pp. 721-738, 2013.

[21] F. Dellaert, "Factor graphs and GTSAM: a hands-on introduction," *Technical Report GT-RIM-CP&R-2012-002*.

[22] L. Génevé, O. Kermorgant, É. Laroche, "Limits of trilateration-based sensor placement algorithms," *IEEE Sensors Applications Symposium*, 2017.

[23] L. Zwirello, T. Schipper, M. Harter and T. Zwick, "UWB localization system for indoor applications: concept, realization and analysis," *Journal of Electrical and Computer Engineering*, vol. 12, 2012.

[24] Z. Arjmandi, J. Kang, K. Park, and G. Sohn, "Benchmark dataset of ultra-wideband radio based UAV positioning," *IEEE International Conference on Intelligent Transportation Systems (ITSC)*, 2020.